

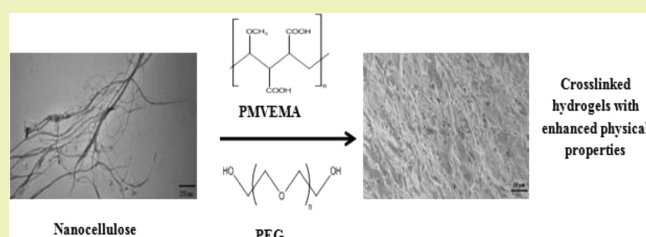
Hydrogels Prepared from Cross-Linked Nanofibrillated Cellulose

Sandeep S. Nair,[†] J. Y. Zhu,[§] Yulin Deng,[‡] and Arthur J. Ragauskas^{†,*}[†]School of Chemistry and Biochemistry, Georgia Institute of Technology, 500 10th Street NW, Atlanta, Georgia 30332, United States[‡]School of Chemical and Biomolecular Engineering, Georgia Institute of Technology 500 10th Street NW, Atlanta, Georgia 30332, United States[§]Forest Products Laboratory, Forest Service, U.S. Department of Agriculture, One Gifford Pinchot Drive, Madison, Wisconsin 53726, United States

Supporting Information

ABSTRACT: Nanocomposite hydrogels were developed by cross-linking nanofibrillated cellulose with poly(methyl vinyl ether-co-maleic acid) and polyethylene glycol. The cross-linked hydrogels showed enhanced water absorption and gel content with the addition of nanocellulose. In addition, the thermal stability, mechanical strength, and modulus increased with an increase in the amount of nanocellulose in hydrogels, and this can be attributed to efficient cross-linking between the nanocellulose and the matrix. The addition of softwood nanocellulose showed much higher strength and strain properties in the hydrogels than with the addition of hardwood nanocellulose. The enhanced physical properties confirm that in situ cross-linking of nanofibrillated cellulose with the matrix polymer forms hydrogels that are not just blends of starting materials but are distinctively unique and formed by cross-linking interactions between the filler and matrix.

KEYWORDS: Nanofibrillated cellulose, Hydrogels, Water absorption, Gel content, Thermal stability, Tensile property



INTRODUCTION

Hydrogels are three-dimensional cross-linked linear or branched polymers with the ability to absorb and retain significant amount of water without being dissolved.¹ Major uses of hydrogels have occurred where mechanical properties are not decisive, such as in biomedical applications² and tissue engineering³ and for biosensors⁴ and drug delivery.⁵ Recently, extensive studies are underway in developing nanocomposite hydrogels. At the nanoscale, the particles have a large surface area for a given volume, and they behave in a different way from those of the bulk material.⁶ Because of their large surface area, nanoparticles interact with polymer chain movement and thereby manipulate the matrix properties.⁷ Being evenly distributed in polymer matrices, these particles can increase the mechanical performance, thermal stability, and barrier properties of the resulting composites.^{8,9} Thus, the use of nanoparticles in hydrogels can enhance the physical properties and thereby the potential for a wide spectrum of applications.

Nanocomposite hydrogels using exfoliated clay nanoparticles have been extensively studied and have shown exceptional mechanical properties.^{10,11} Hydrogels based on poly (acrylic acid)-graphene oxide¹² and poly (acrylamide)-silica¹³ have shown better mechanical performance due to strong interactions between these nanoparticles and polymer matrices. Because of growing environmental awareness and legislative requirements, the biodegradability of hydrogels together with the degradation rate can provide additional value to the developed materials. In recent years, there has been a high focus on research and

design of cellulose-based hydrogels, which combines biodegradability with smart stimuli sensitive behavior.¹ Cellulose is the most abundant polymer in nature, accounting for approximately 40% of the lignocellulosic biomass. The ability of cellulose to absorb enormous amounts of water has prompted the large use of cellulose in various hydrogels. Many factors affect the ability of cellulose to absorb water. The most important being the crystallinity, amorphous regions, total surface area, and pore volume.¹⁴ Much of the moisture uptake occurs in the amorphous or disordered regions of cellulose.¹⁵ Cellulose with high crystallinity showed lower moisture uptake at relative humidity less than 75%, while highly crystalline nanocellulose obtained from *Cladophora* green algae showed high moisture uptake at higher humidities. The increase in water uptake can be associated to the increase in surface area and pore volume of the algal nanocellulose.¹⁴ Nanofibrillated cellulose (NFC) or cellulose microfibrils constitute the smallest fibrous component of cellulose fibers that have diameters in the range of 2–20 nm and lengths up to several micrometers depending on their origin.¹⁶ Owing to the abundance, large surface area, water retention value, transparency, and sustainability aspects, NFC has been considered a prime candidate for many applications in the material science field.¹⁷ Not only produced by plants, cellulose can also be produced by bacteria. The bacterially synthesized nanocellulose

Received: November 4, 2013

Revised: December 17, 2013

Published: January 3, 2014

(BNC) possess a supramolecular structure quite different from plant nanocellulose. The BNC strongly interact with water, and it has been shown that only 10% of the 99% water in BNC hydrogels behave as free bulk water; the rest of the water is strongly bound to cellulose.¹⁸ The use of BNC was found to increase the swelling capacity of hydrogels, and it also increased the thermal stability as more interpolymer interactions were present between the high surface area nanocellulose and poly(acrylic acid).¹⁹ In recent years, there has been great interest in the use of NFC in enhancing the physical properties of hydrogels. Results from studies showed that nanocomposite hydrogels reinforced with NFC may be viable as nucleus pulposus implants due to their adequate swelling ratio and increased mechanical properties.²⁰ The use of a gelatin matrix cross-linked with oxidized cellulose nanowhiskers was found to produce hydrogels with superior mechanical properties.²¹ Compared with cellulose whiskers, NFC has the advantage of a high aspect ratio and can form strong physical entanglements and networks in composites. These features make the gels much stronger than in the case when the network is formed only because of weak hydrogen bonds between water and fibrils.²²

Poly(methyl vinyl ether-co-maleic acid) (PMVEMA)–polyethylene glycol (PEG) hydrogels have been investigated for their potential application in controlled drug delivery systems.²³ Recently, there has been great interest in expanding its use with cellulosic materials. Barcus and Bjorkquist²⁴ developed a transesterification approach for cross-linking PMVEMA–PEG matrix with cellulose fibers without the need to use a metal catalyst for grafting. The resulting material achieved high water absorbencies. Recently, Goetz et al.²⁵ reported the preparation and characterization of nanocomposite hydrogels from cellulose whiskers cross-linked with PMVEMA and PEG. The resultant nanocomposites showed high water absorption without being dissolved or losing its integrity. Likewise, Pan and Ragauskas²⁶ examined the effects of fiber length, cross-linking reaction time, and dosage of PMVEMA on water absorption and retention for PVEMA–PEG/cellulose fiber hydrogels. The aim of this study is to develop nanofibrillated cellulose cross-linked PMVEMA–PEG hydrogels and to investigate the effect of different concentrations of NFC on its physical properties. Compared to softwood cellulose fiber-based hydrogels, very limited studies have been conducted based on hardwood cellulose fibers. Hardwood fibers are known to have thicker cell walls, shorter fibers, and different chemical composition than softwood fibers.²⁷ So, this study also investigates the difference in physical properties of hardwood and softwood NFC cross-linked PMVEMA–PEG matrices.

EXPERIMENTAL SECTION

Materials. Elementally chlorine-free (ECF) bleached kraft softwood (Loblolly pine) pulp and kraft hardwood (Eucalyptus) pulp were commercial samples. The chemical composition of the softwood pulp was 79.6% glucan, 9.2% xylan, and $0.7 \pm 0.1\%$ Klason lignin and that for the hardwood was 78.1% glucan, 15.3% xylan, and $0.7 \pm 0.1\%$ Klason. PMVEMA (MW: 1,200,000) is a water-soluble polymer that was supplied by ISP Technologies Inc. (Wayne, NJ, U.S.A.). PEG with a MW of 8500–11500 was purchased from Sigma-Aldrich (St. Louis, MO, U.S.A.). All other chemicals were ACS reagent grade obtained from Sigma-Aldrich.

Preparation of NFC. Bleached kraft pulp at 2% solids was soaked in deionized water for 24 h and then disintegrated using a lab disintegrator (TMI, Ronkonkoma, NY, U.S.A.) for 10,000 revolutions. It was then nanofibrillated using a SuperMassColloider (MKZA6-2, Masuko Sangyo Co., Ltd., Japan) at 1500 rpm for 6 h. Pulp was fed continuously

to the colloid consisting of two stone grinding disks positioned on top of each other. The gap between the two disks was adjusted to $-100 \mu\text{m}$. The zero gap corresponds to the starting point where the two disks just contact each other before loading pulp. The presence of pulp between the disks ensured that there is no direct contact between the disks. The NFC was treated with Kathon CP/ICP II (Rohm and Haas company, Bellefonte, PA, U.S.A.) at a dose of $10 \mu\text{L}/\text{mL}$ of fibrillated suspension in order to avoid mold growth.

Preparation of NFC-Based Hydrogels. The procedure for preparing the PMVEMA–PEG/NFC hydrogels was already described elsewhere.²⁵ In brief, a 6.7:1 mass ratio of PMVEMA:PEG (3.85 g) was added to distilled water (40.00 mL) preheated to 68°C and acidified to pH 2 with 1.00 N HCl. The reaction mixture was then thoroughly mixed with different concentrations of NFC. Five compositions were prepared using both softwood and hardwood NFC. They were classified based on the percent NFC mass content in the resulting hydrogels. The amount of NFC in the resultant hydrogels were 25%, 50%, 75%, and 100% and were named 25SWNFC, 50SWNFC, 75SWNFC, and 100SWNFC for softwood. For the hardwood, they were named as 25HWNFC, 50HWNFC, 75HWNFC, and 100HWNFC. Each PMVEMA–PEG/NFC mixture was solution cast onto glass Petri dishes, air-dried, and then cured at 135°C for 6.5 min. Also, control films of PMVEMA–PEG with 25% or 50% NFC were also prepared using the same method as the cross-linked nanocomposite hydrogels with the exception of not being cured. The films were allowed to cool to room temperature and stored in a desiccator at 50% relative humidity for one week prior to testing.

Characterizations. Transmission electron microscopy (TEM) images were acquired on a JEOL 100CXII TEM (JEOL USA, Inc., Peabody, MA, U.S.A.) using an acceleration voltage of 100 kV. The TEM samples were prepared by placing a drop of a diluted suspension of NFC on carbon-coated grids followed by staining with a 0.5 wt % uranyl acetate solution.

Scanning electron microscopic (SEM) images of the surface morphology of lyophilized noncross-linked and cross-linked hydrogels were studied by a scanning electron microscope (LEO 1530 SEM, Carl Zeiss NTS, Peabody, MA, U.S.A.) at 15 kV. Hydrogels were quickly frozen using liquid nitrogen and then mounted on an aluminum stub and dried. Also, the morphology of swollen hydrogels was studied. The hydrogel samples were immersed in water for one day to attain an equilibrium moisture content. Swollen hydrogels were quickly frozen using liquid nitrogen, freeze-dried, and then mounted on an aluminum

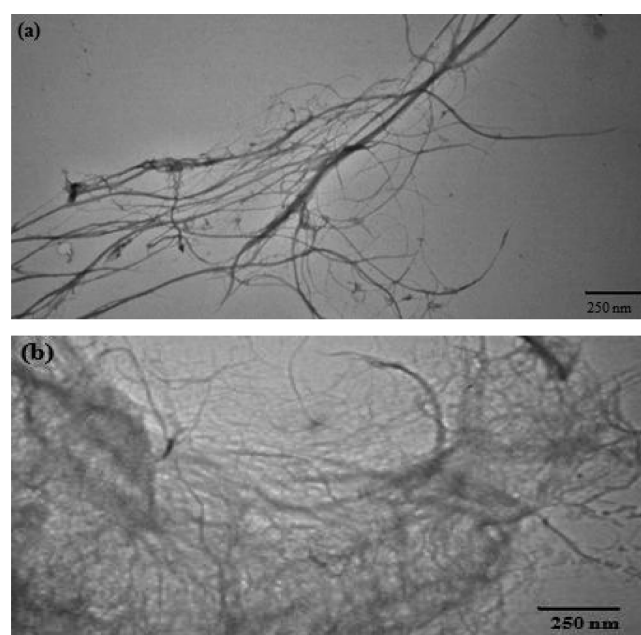


Figure 1. TEM images of NFC: (a) softwood and (b) hardwood.

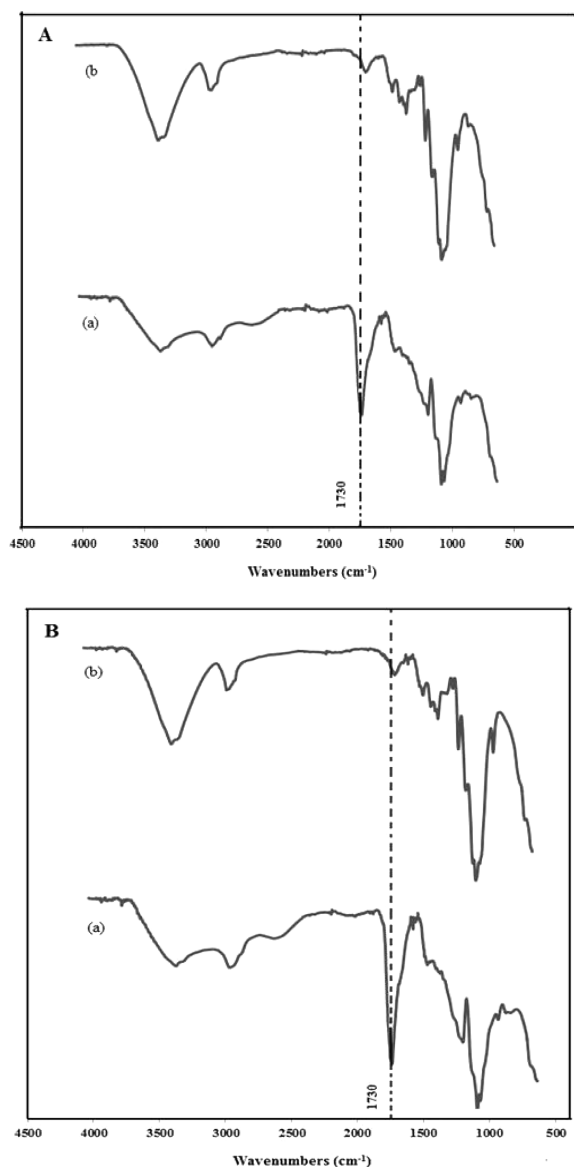


Figure 2. FTIR comparative spectra of (A) are (a) 25SWNFC and (b) 100SWNFC and of (B) are (a) 25HWNFC and (b) 100HWNFC.

stub and dried. Surfaces of all the samples were coated with gold to provide adequate conductivity.

Fourier transform infrared spectra (FTIR) were recorded on a Perkin-Elmer Spectrum 100 (PerkinElmer, Waltham, MA, U.S.A.) working in transmission mode. Spectra were recorded between 500 and 4000 cm^{-1} at a resolution of 4 cm^{-1} , and 32 scans were collected for each spectrum.

X-ray diffraction (XRD) analyses for the softwood and hardwood nanocellulose were carried out using a PANalytical X Ray diffractometer (PANalytical, Inc., Westborough, MA, U.S.A.) using a Cu $K\alpha$ source ($\lambda = 0.154 \text{ nm}$) with a 2θ range from 10–26° with a scanning step of 0.033°/scan.

$$\% \text{ Crystallinity} = \frac{I_{\text{cr}}}{(I_{\text{cr}} + I_{\text{am}})} \times 100 \quad (1)$$

where I_{cr} is the intensity of the crystalline peak, and I_{am} is the intensity of the amorphous peak

Water Absorption Study. The hydrogel samples used for the water absorption study were circular discs of diameter 25.4 mm immersed in an excess of deionized water at room temperature. Three samples from each composition were used. The samples were removed

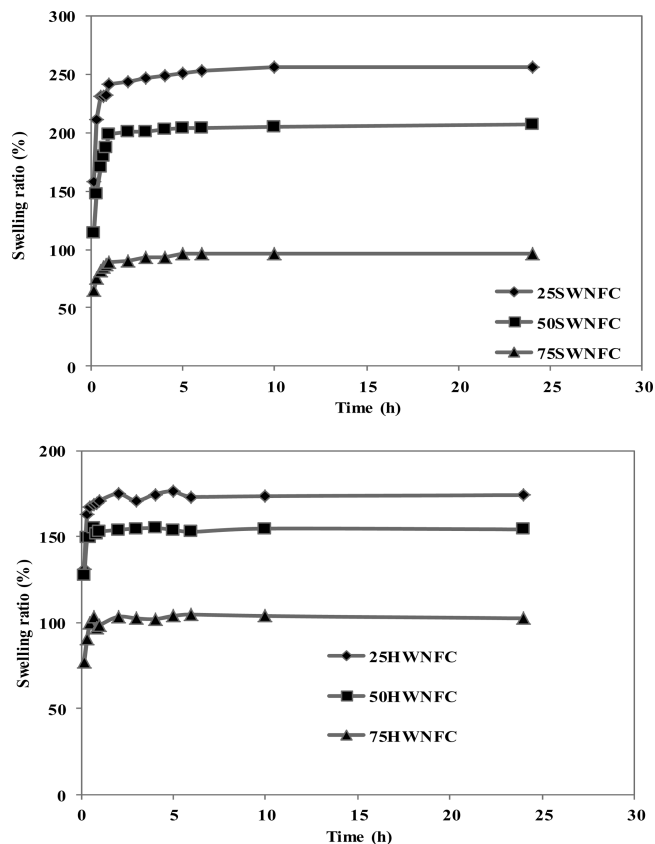


Figure 3. Swelling ratio of cross-linked nanocomposite hydrogels with (a) softwood nanocellulose and (b) hardwood nanocellulose.

from water at various intervals and placed on a blotting paper, and a second sheet of blotting paper was placed on the top of the sample. The excess water was removed by moving a metal roller weighing $10 \pm 0.5 \text{ kg}$ once back and once forward over the blotting papers containing the sample in-between without exerting any addition pressure on the roller. The sample was then weighed to determine the water uptake. The water uptake was determined according to the following equation

$$\text{Water uptake} = \frac{(W_2 - W_1)}{W_1} \times 100 \quad (2)$$

where W_1 is the weight of the NFC hydrogel composite before immersion, and W_2 is the weight of the NFC hydrogel composite after immersion.

This immersion process was continued until equilibrium swelling was reached which was indicated by constant weight.

Gel Content. Gel content of the prepared films was measured using ASTM standard 2765. Three samples from each composition was cycled with water for 24 h, after which, the samples were removed, dried to constant weight, and weighed. Gel content was calculated with the following

$$\text{Gel fraction (\%, W/W)} = 100 - \left[\frac{(W_1 - W_2)}{W_1} \times 100 \right] \quad (3)$$

where W_1 is the weight of the NFC-based hydrogel before extraction, and W_2 is the weight of the NFC-based hydrogel after extraction.

Thermogravimetric Analysis (TGA). TGA of the prepared films were performed on a TA TGA Q50 (TA Instruments, New Castle, DE, U.S.A.). Samples (8–10 mg) were heated from room temperature to 600 °C at a rate of 10 °C/min.

Mechanical Testing. The tensile measurements were performed on a BOSE ELF3200 (Bose Corp., Eden Prairie, MN, U.S.A.) with a 100 N load cell. Rectangular shaped strips (0.10–0.30 mm thickness)

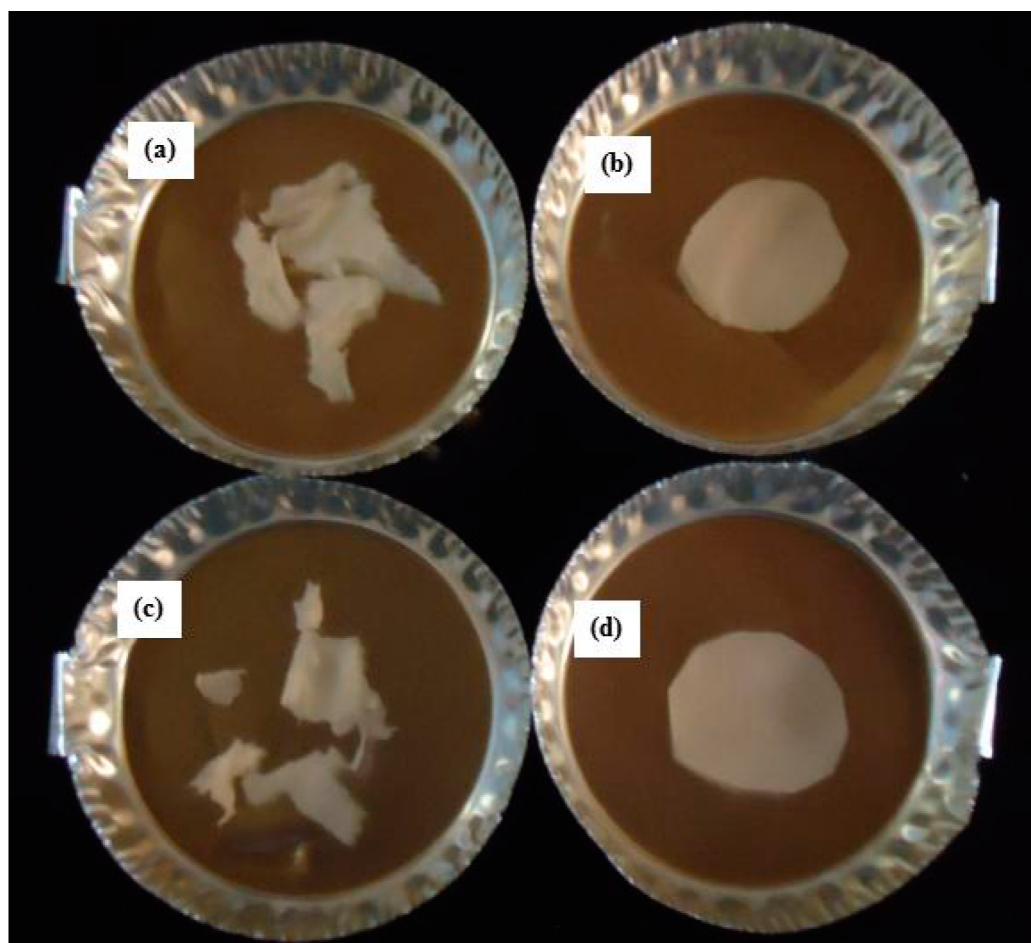


Figure 4. Difference in structures of cross-linked and noncross-linked hydrogels after water immersion: (a) noncross-linked 2SSWNFC, (b) cross-linked 2SSWNFC, (c) noncross-linked 2SHWNFC, and (d) cross-linked 2SHWNFC.

were cut from the films. The gauge length was 20 mm, and a strain rate of 5 mm/min was applied. Five specimens for each experimental condition were prepared and sampled for mechanical testing. The error in the measurements was reported as the standard deviation.

RESULTS AND DISCUSSION

Figure 1 shows the TEM images of nanofibrillated samples for softwood and hardwood. The average diameter of the nanofibrils was found to be 17.6 ± 9.5 and 14.3 ± 8.7 nm for softwood and hardwood, respectively. Figure 2 shows the FTIR spectrum for the pure NFC and cross-linked PVMEVA-PEG/NFC hydrogels. The cross-linking reaction between PVMEVA, PEG, and cellulose fibers occurs through the transesterification reactions between the carboxylic acid groups of PMVEMA and the hydroxyl groups of PEG and nanofibrillated cellulose.^{25,26} Strong peaks at 1730 cm^{-1} shows evidence of esterification between the hydroxyl group of nanocellulose and PEG with the carboxyl groups of PMVEMA.²⁶ Figure S1 of the Supporting Information shows the schematic representation of the cross-linking reaction chemistry of PMVEMA, PEG, and NFC.

The water sorption curves for the nanocomposite hydrogels are given in Figure 3. The 100% nanocellulose films and 100% PMVEMA-PEG films did not retain structural integrity after 24 h water absorption experiments. However, the cross-linked nanocomposite hydrogels swelled in water and retained their film structure. Table S1 of the Supporting Information shows equilibrium water uptake during different time periods. It was

found that both softwood and hardwood nanocomposite films almost attained high swelling within 1 h of immersion, and thereafter, hydrogels did not show much increase in water uptake with further immersion. At equilibrium, the 2SSWNFC hydrogels absorbed a higher amount of water (256.2%) compared to both 50SSWNFC (206.3%) and 75SSWNFC (96.3%) hydrogels. At equilibrium, the 2SHWNFC (174.2%) and 50SHWNFC (154.2%) hydrogels absorbed less amounts of water at equilibrium compared to softwood. There was little difference in water absorption for the 75% nanocellulose containing hydrogels between the softwood and hardwood NFC. It has been shown that crystallinity of the cellulose plays a major role in the interaction between celluloses and water as most of the moisture uptake occurs in the bulk of disordered regions of cellulose.^{14,15} In our study, the average percent crystallinity obtained by the X-ray diffraction method was 74.0% and 72.0% for softwood and hardwood nanocellulose, respectively. From Figure 3 and Table S1 of the Supporting Information, it was quite evident that the water absorption decreased with the amount of nanocellulose. The decrease in water uptake with the increase in nanocellulose can be attributed to the increase in cross-linking between the PVMEVA and NFC with the increase in amount of NFC. More cross-linking could result in fewer numbers of free carboxylic groups available for hydration.²⁸

The noncross-linked control samples were completely disintegrated during the process of absorption of excess water from the hydrogels after 24 h of immersion. Figure 4 shows the

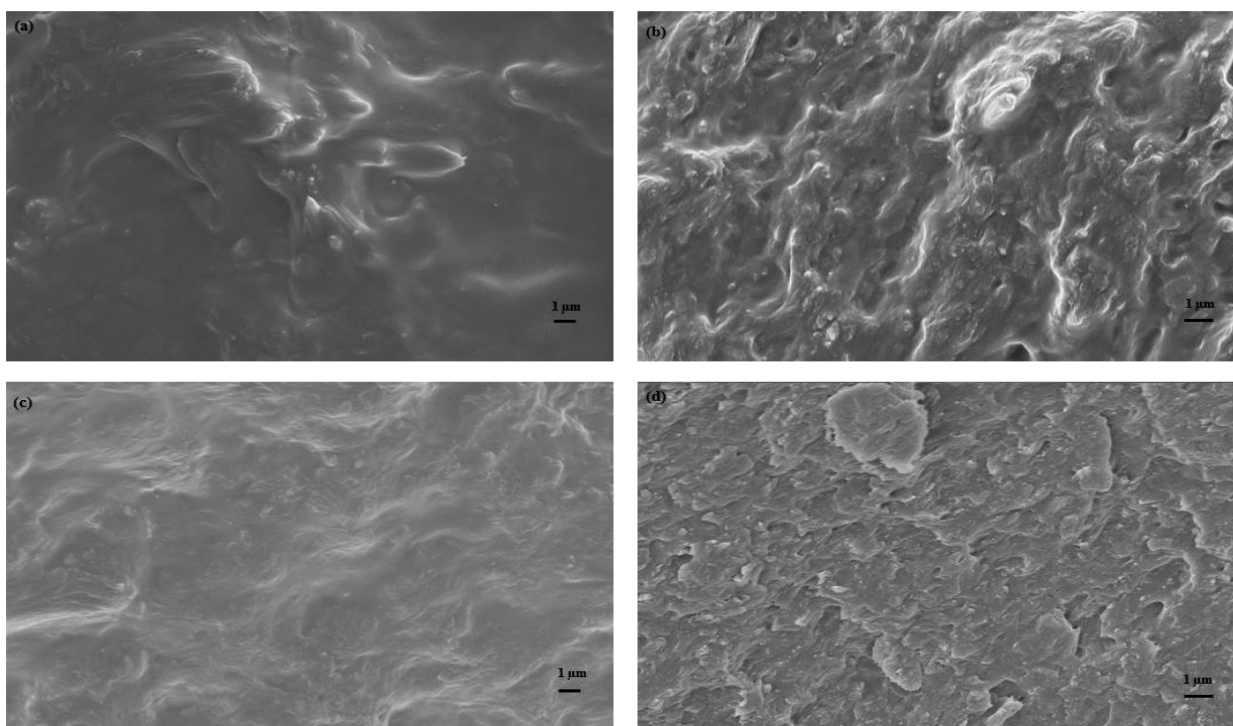


Figure 5. SEM images of fracture surfaces of nonswollen hydrogels: (a) noncross-linked 25SWNFC, (b) cross-linked 25SWNFC, (c) noncross-linked 25HWNFC, and (d) cross-linked 25HWNFC.

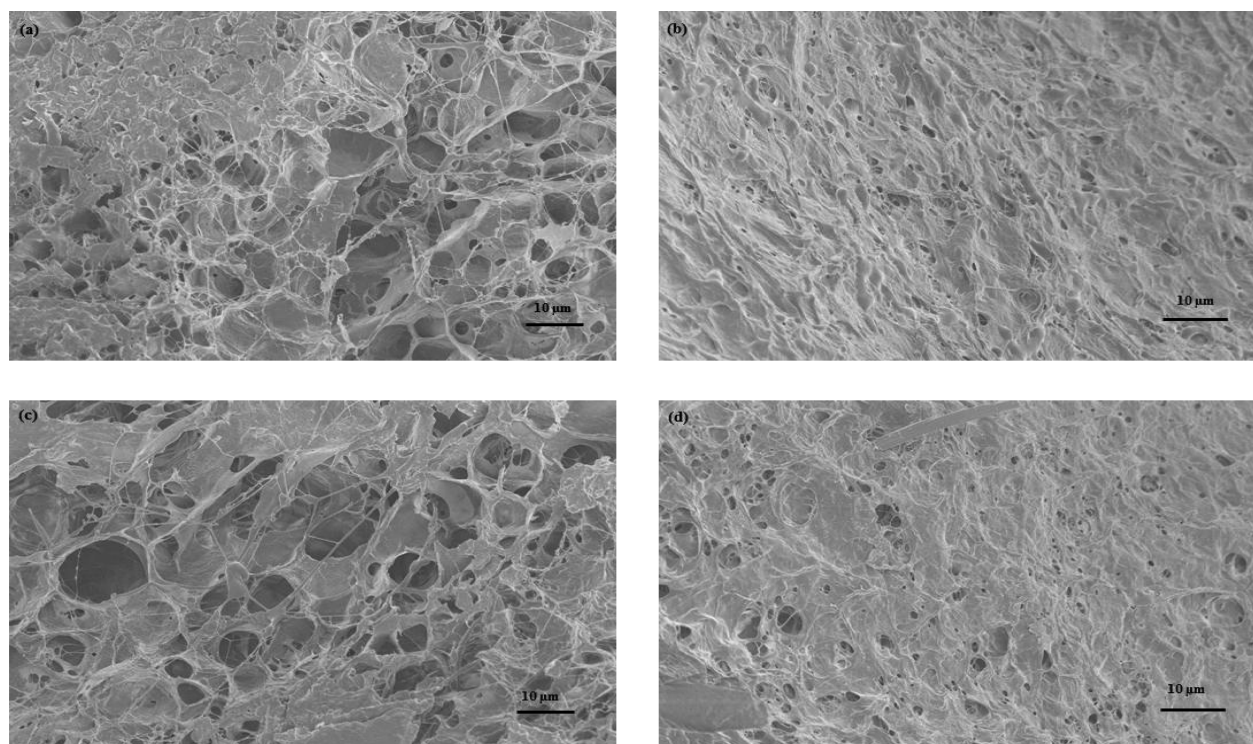


Figure 6. SEM images of fracture surfaces of swollen hydrogels: (a) noncross-linked 25SWNFC, (b) cross-linked 25SWNFC, (c) noncross-linked 25HWNFC, and (d) cross-linked 25HWNFC.

difference in structures of the uncured sample and the cured sample after water immersion. The thermally initiated cross-linking between the carboxylic acid groups of PMVEMA and the hydroxyl groups of PEG and NFC during the curing process maintained the film structure of the hydrogels. Figure 5 shows the SEM images of the fracture surface of nonswollen

hydrogels. The cross section of the cross-linked samples shows a rougher surface than the noncross-linked samples. The presence of a cross-link network has enabled the samples to be stretched to a greater extent before failure, which resulted in more matrix tearing.²⁹ Figure 6 shows the morphology of swollen hydrogels. Noncross-linked samples showed a relatively

open structure with pores of various sizes. However, cross-linking affected the openness of the structure, and the pore size became much smaller.²¹ To further confirm the presence of cross-linking, the gel contents of the prepared hydrogels were determined using the Soxhlet extraction method, and these values are shown in Table 1. The percent gel content was

Table 1. Gel Content of Cross-Linked and Noncrosslinked Nanocomposite Hydrogel

sample	gel content (%)
2SSWNFC	36.2
noncross-linked 2SSWNFC	no gel
50SWNFC	58.2
75SWNFC	84.8
noncross-linked 75HWNFC	48.1
2SHWNFC	19.4
noncross-linked 2SHWNFC	no gel
50HWNFC	60.8
75HWNFC	80.4
noncross-linked 75HWNFC	43.0

directly proportional to the nanocellulose content used in the hydrogels supporting the fact that cross-linking between the PVEMA and NFC increased with the increase in the amount of NFC. Although, the 25% cross-linked softwood nanocellulose containing films showed higher gel content than the 25% cross-linked hardwood nanocellulose films, there was not much difference in gel content for the higher cross-linked nanocellulose (50% and 75%) containing hydrogels between the softwood and hardwood. The noncross-linked 25% nanocellulose control hydrogels did not show any gel content at all, while the noncross-linked 75% samples showed significantly less gel content than the cross-linked 75% samples, which further shows the importance of cross-linking in maintaining a hydrogel structure.

The thermal stability and degradation behavior of cross-linked nanocomposite hydrogels is a very important parameter in determining their potential applications. The TGA results showed two important temperature characteristics, namely, T_{onset} , defined as the temperature where the sample weight was 93% of the sample mass at 105 °C, and T_{max} , the maximum value on the derivative weight curve, which is the temperature at which the degradation rate is fastest. Figure 7a shows the decomposition of the PMVEMA–PEG (0% NFC) films. The T_{onset} of degradation was 147 °C for the PVEMA–PEG films. The derivative weight curve showed three distinct peaks with T_{max} at 160, 250, and 390 °C, respectively. The first peak is associated with the dehydration of the diacids of the PVEMA. The second peak is associated with the combined decomposition of PVEMA and PEG, and the final peak is attributed to the polymer chain degradation. Figure 7b shows the degradation behavior for the pure NFC for both hardwood and softwood. The T_{onset} of degradation for softwood and hardwood NFC films were 264 and 267 °C, respectively. The derivative weight curve showed a distinct peak with T_{max} at 321 °C for softwood and hardwood nanocellulose. These results indicate that nanocellulose were more thermally stable than the PVEMA–PEG matrix.

Figure 8 shows the thermal degradation behavior of the NFC cross-linked PMVEMA–PEG matrix. Table 2 shows the T_{onset} and T_{max} values. The thermal stability of the matrix was substantially increased with the addition of nanocellulose as seen by the T_{onset} values. The increase in the decomposition temperature

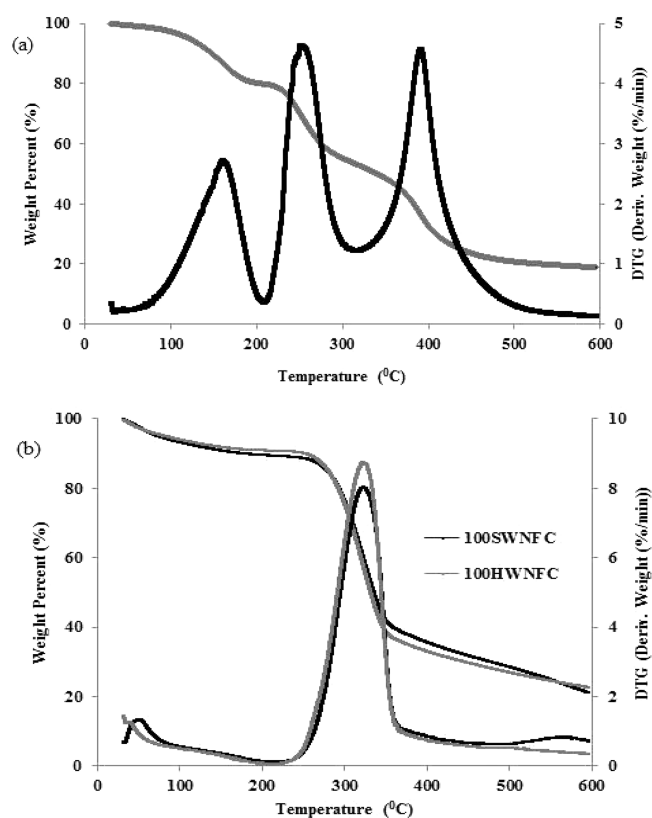


Figure 7. TGA and DTG of (a) PMVEMA–PEG matrix and (b) 100 NFC.

with the increase in nanocellulose can be attributed to the efficient cross-linking between the NFC and the matrix. Also, it is quite evident from the data (Table 2) that there is a shift in TGA and DTG curves with the addition of nanocellulose. The T_{max} values for different peaks of PMVEMA–PEG films are quite different from the cross-linked hydrogels, which indicates that there is strong interaction between the PMVEMA–PEG matrix and nanocellulose. There was no significant difference in thermal stability between the softwood and hardwood nanocomposite hydrogels.

The materials exhibit typical behavior as a function of strain, consisting of an initial elastic region followed by a strain-hardening plastic region. Associated mechanical property data are provided in Table 3. The NFC cross-linked PMVEMA–PEG hydrogels showed substantial increase in mechanical properties than those of pure PMVEMA–PEG hydrogels. As the nanocellulose content increased, the strength and modulus increased. According to the literature, the increase in concentration of nanocellulose always increases the strain in resulting films.¹⁶ However, in our study, the strain decreased with the increase in nanocellulose content. This can be attributed to the increase in cross-linking between the nanocellulose and matrix as evidenced by the increase in gel content.³⁰ In the case of the different nanocellulose furnish used, the addition of softwood nanocellulose showed much higher strength and strain properties than with the addition of hardwood nanocellulose. From the TEM images, it was observed that there was no significant difference in the average fiber diameter among the different nanocellulose. It is possible that the hardwood fibrils are shorter when compared to softwood fibrils after nanofibrillation, which could explain the lower

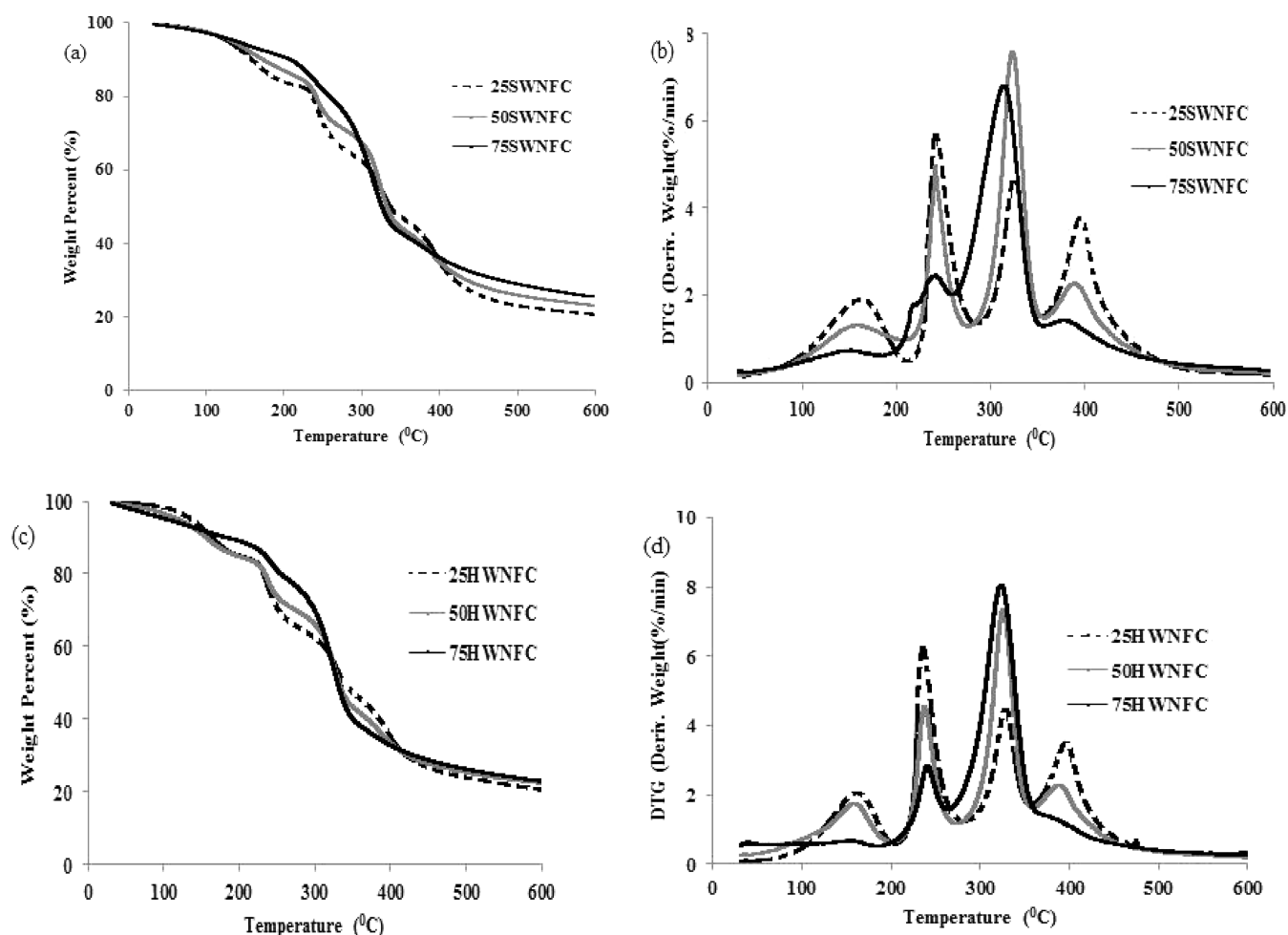


Figure 8. (a) TGA of softwood hydrogels, (b) DTG of softwood hydrogels, (c) TGA for hardwood hydrogels, and (d) DTG for hardwood hydrogels.

Table 2. T_{onset} and T_{max} Values for the Softwood and Hardwood Crosslinked Nanocomposite Hydrogels

sample	T_{onset} (°C)	1 st peak, T_{max} (°C)	2 nd peak, T_{max} (°C)	3 rd peak, T_{max} (°C)	4 th peak, T_{max} (°C)
25SWNFC	154	160	240	324	394
50SWNFC	168	157	240	321	388
75SWNFC	204	150	240	313	376
25HWNFC	156	161	234	326	394
50HWNFC	170	157	236	324	387
75HWNFC	209	153	239	321	—

mechanical properties.¹⁶ The shorter fibers yield more ends per unit volume, thereby more defects per unit volume, and these fibers are rigid and easy to pull out from the aggregation of fibers making the films more brittle than the longer fibers.³¹

In summary, the in situ co-cross-linking of NFC with the PVMEVA-PEG matrix led to the development of nanocomposite hydrogels with enhanced physical properties. The cross-linked nanocomposite hydrogels swelled in water and retained their film structure. The cross-linked hydrogels attained high water absorption at 25% nanofibrillated cellulose. The water absorption decreased with the increase in nanocellulose, and that can be attributed to the increase in cross-linking density between the polymer and nanocellulose. The noncross-linked control samples completely disintegrated during the process of water absorption and did not retain their hydrogel structure. The increase in percent gel content was directly proportional to nanocellulose content in the hydrogels.

Table 3. Mechanical Property Data

sample	tensile strength (MPa)	E-modulus (GPa)	strain (%)
PVEMA-PEG	2.64 ± 0.33	0.23 ± 0.70	0.82 ± 0.01
25SWNFC	14.81 ± 1.42	0.60 ± 0.15	3.4 ± 0.40
50SWNFC	20.12 ± 0.81	0.75 ± 0.22	2.85 ± 0.02
75SWNFC	31.38 ± 0.20	1.60 ± 0.07	2.07 ± 0.06
25HWNFC	9.44 ± 0.50	0.46 ± 0.10	3.0 ± 0.40
50HWNFC	12.07 ± 2.0	0.77 ± 0.12	2.66 ± 0.08
75HWNFC	20.41 ± 1.40	1.65 ± 0.23	1.6 ± 0.30

The noncross-linked control hydrogels with 25% nanocellulose did not show any gel content at all, while the noncross-linked hydrogels with 75% nanocellulose showed significantly less gel content than the cross-linked samples with 75% nanocellulose, which further shows the importance of cross-linking in maintaining

a hydrogel structure. The thermal stability, mechanical strength, and modulus increased with the increase in the amount of nanocellulose in cross-linked hydrogels. Decrease in strain with the increase in nanocellulose can be attributed to an effective increase in cross-linking within the hydrogels. Although, there was substantial difference in the water absorption and gel content for 25% nanocellulose hydrogels between softwood and hardwood, the difference became insignificant with the increase in the amounts of nanocellulose. The addition of softwood nanocellulose showed much higher strength and strain properties in the hydrogels than with the addition of hardwood nanocellulose. There was not any significant difference in thermal stability between the softwood and hardwood hydrogels.

■ ASSOCIATED CONTENT

● Supporting Information

Schematic representation of the cross-linking reaction chemistry of poly(methyl vinyl ether-co-maleic acid) (PMVEMA), polyethylene glycol (PEG), and nanofibrillated cellulose (NFC) and table showing equilibrium water uptake during different time periods. This material is available free of charge via the Internet at <http://pubs.acs.org>.

■ AUTHOR INFORMATION

Corresponding Author

*Telephone: 01-404-8949701. Fax: 01-404-8944778. E-mail: arthur.ragauskas@chemistry.gatech.edu.

Notes

The authors declare the following competing financial interest(s): Ragauskas receives funding in this field.

■ ACKNOWLEDGMENTS

This work was partially supported by the USDA Forest Service R&D special funding on Cellulose Nano-Materials (2012).

■ REFERENCES

- (1) Sannino, A.; Demitri, C.; Madaghiele, M. Biodegradable cellulose-based hydrogels: Design and applications. *Materials* **2009**, *2* (2), 353–373.
- (2) Murthy, P. S. K.; Mohan, Y. M.; Varaprasad, K.; Sreedhar, B.; Raju, K. M. First successful design of semi-IPN hydrogel–silver nanocomposites: A facile approach for antibacterial application. *J. Colloid Interface Sci.* **2008**, *318* (2), 217–24.
- (3) Kim, J.; Lee, K.; Hefferan, T. E.; Currier, B. L.; Yaszemski, M. J.; Lu, L. Synthesis and evaluation of novel biodegradable hydrogels based on poly(ethylene glycol) and sebacic acid as tissue engineering scaffolds. *Biomacromolecules* **2008**, *9* (1), 149–57.
- (4) Adhikari, B.; Majumdar, S. Polymers in sensor applications. *Prog. Polym. Sci.* **2004**, *29* (7), 699–766.
- (5) Zhang, X.; Yang, Y.; Chung, T. The influence of cold treatment on properties of temperature-sensitive poly(N-isopropylacrylamide) hydrogels. *J. Colloid Interface Sci.* **2002**, *246* (1), 105–11.
- (6) Hussain, F.; Hojjati, M.; Okamoto, M.; Gorga, R. E. Polymer-matrix nanocomposites, processing, manufacturing, and applications: an overview. *J. Compos. Mater.* **2006**, *40* (17), 1511–1575.
- (7) Schaefer, D. W.; Justice, R. S. How nano are nanocomposites? *Macromolecules* **2007**, *40* (24), 8501–8517.
- (8) Alexandre, M.; Dubois, P. Polymer-layered silicate nanocomposites: preparation, properties and uses of a new class of materials. *Mater. Sci. Eng., R* **2000**, *28*, 1–63.
- (9) Tjong, S. C. Novel nanoparticle-reinforced metal matrix composites with enhanced mechanical properties. *Adv. Eng. Mater.* **2007**, *9* (8), 639–652.
- (10) Haraguchi, K.; Takehisa, T. Nanocomposite hydrogels: a unique organic-inorganic network structure with extraordinary mechanical, optical, and swelling/de-swelling properties. *Adv. Mater.* **2002**, *14* (16), 1120–24.
- (11) Haraguchi, K.; Takehisa, T.; Fan, S. Effects of clay content on the properties of nanocomposite hydrogels composed of poly(N-isopropylacrylamide) and clay. *Macromolecules* **2002**, *35* (27), 10162–10171.
- (12) Shen, J.; Yan, B.; Li, T.; Long, Y.; Li, N.; Ye, M. Mechanical, thermal and swelling properties of poly(acrylic acid)-graphene oxide composite hydrogels. *Soft Matter* **2012**, *8* (6), 1831–1836.
- (13) Yang, J.; Han, C.; Duan, J.; Xu, F.; Sun, R. Interaction of silica nanoparticle/polymer nanocomposite cluster network structure: Revisiting the reinforcement mechanism. *J. Phys. Chem. C* **2013**, *117* (16), 8223–8230.
- (14) Mihranyan, A.; Llasgostera, A. P.; Karmhag, R.; Stromme, M.; Ek, R. Moisture sorption by cellulose powders of varying crystallinity. *Int. J. Pharm.* **2004**, *269*, 433–442.
- (15) Howsman, J. A. Water sorption and the poly-phase structure of cellulose fibers. *Text. Res. J.* **1949**, *19*, 152–162.
- (16) Stelte, W.; Sanadi, A. R. Preparation and characterization of cellulose nanofibers from two commercial hardwood and softwood pulps. *Ind. Eng. Chem. Res.* **2009**, *48* (24), 11211–219.
- (17) Abraham, E.; Deepa, B.; Pothan, L. A.; Jacob, M.; Thomas, S.; Cvelbar, U.; Anandjiwala, R. Extraction of nanocellulose fibrils from lignocellulosic fibers: A novel approach. *Carbohydr. Polym.* **2011**, *86* (4), 1468–1475.
- (18) Gelin, K.; Bodin, A.; Gatenholm, P.; Mihranyan, A.; Edwards, K.; Stromme, M. Characterization of water in bacterial cellulose using dielectric spectroscopy and electron microscopy. *Polymer* **2007**, *48*, 7623–7631.
- (19) Johari, N. S.; Ahmad, I.; Halib, N. Comparison study of hydrogels properties synthesized with micro- and nano size bacterial cellulose particles extracted from Nata de coco. *Chem. Biochem. Eng. Q.* **2012**, *26* (4), 399–404.
- (20) Eyholzer, C.; Borges de Couraça, A.; Duc, F.; Bourbon, P. E.; Tingaut, P.; Zimmermann, T.; Manson, J. A. E.; Oskman, K. Biocomposite hydrogels with carboxymethylated, nanofibrillated cellulose powder for replacement of the nucleus pulposus. *Biomacromolecules* **2011**, *12* (5), 1419–1427.
- (21) Dash, R.; Foston, M.; Ragauskas, A. J. Improving the mechanical and thermal properties of gelatin hydrogels cross-linked by cellulose nanowhiskers. *Carbohydr. Polym.* **2013**, *91* (2), 638–645.
- (22) Pääkkö, M.; Ankerfors, M.; Kosonen, H.; Nykaenen, A.; Ahola, S.; Oesterberg, M.; Ruokolainen, J.; Laine, J.; Larsson, P. T.; Ikkala, O.; Lindstroem, T. Enzymatic hydrolysis combined with mechanical shearing and high-pressure homogenization for nanoscale cellulose fibrils and strong gels. *Biomacromolecules* **2007**, *8* (6), 1934–1941.
- (23) Singh, T. R. R.; Woolfson, A. D.; Donnelly, R. F. Investigation of solute permeation across hydrogels composed of poly(methyl vinyl ether-co-maleic acid) and poly(ethylene glycol). *J. Pharm. Pharmacol.* **2010**, *62* (7), 829–837.
- (24) Barcus, R. L.; Bjorkquist, D. W. Poly(methyl vinyl ether-co-maleate) and Polyol Modified Cellulosic Fiber. U.S. Patent 5049235 A, 1991.
- (25) Goetz, L.; Mathew, A. P.; Oksman, K.; Gatenholm, P.; Ragauskas, A. J. A novel nanocomposite film prepared from crosslinked cellulose whiskers. *Carbohydr. Polym.* **2009**, *75* (1), 85–89.
- (26) Pan, S.; Ragauskas, A. J. Preparation of superabsorbent cellulosic hydrogels. *Carbohydr. Polym.* **2012**, *87* (2), 1410–1418.
- (27) Fengel, D.; Wegner, G. *Wood: Chemistry, Ultrastructure, Reactions*; Walter de Gruyter: Berlin and New York, 1984.
- (28) Gulrez, S. K. H.; Al-Assaf, S.; Phillips, G. O. Hydrogels: Methods of Preparation, Characterisation and Applications. In *Progress in Molecular and Environmental Bioengineering - From Analysis and Modeling to Technology Applications*, Angelo Carpi, A., Ed.; InTech: Rijeka, Croatia, **2011**; ISBN: 978-953-307-268-5; DOI: 10.5772/24553; <http://www.intechopen.com/books/progress-in-molecular-and-environmental-bioengineering-from-analysis-and-modeling-to-technology-applications/hydrogels-methods-of-preparation-characterisation-and-applications>.

(29) Ismail, H.; Nasir, M. N. Dynamic vulcanization of rubberwood-filled polypropylene/natural rubber blends. *Polym. Test.* **2001**, *20*, 819–823.

(30) Goetz, L.; Foston, M.; Mathew, A. P.; Oksman, K.; Ragauskas, A. J. Poly(methyl vinyl ether-co-maleic acid)-polyethylene glycol nanocomposites cross-linked in situ with cellulose nanowhiskers. *Biomacromolecules* **2010**, *11*, 2660–2666.

(31) Nakagaito, A. N.; Yano, H. The effect of morphological changes from pulp fiber towards nano-scale fibrillated cellulose on the mechanical properties of high-strength plant fiber based composites. *Appl. Phys. A: Mater. Sci. Process* **2004**, *78* (4), 547–552.